Supplementary material

Proteome-wide survey of the autoimmune target repertoire in autoimmune polyendocrine syndrome type 1

*Nils Landegren[1,2], Donald Sharon[3,4], Eva Freyhult[2,5,6,], Åsa Hallgren[1,2], Daniel Eriksson[1,2], Per-Henrik Edqvist[7], Sophie Bensing[8], Jeanette Wahlberg[9], Lawrence M. Nelson[10], Jan Gustafsson[11], Eystein S Husebye[12], Mark S Anderson[13], Michael Snyder[3], Olle Kämpe[1,2]

Nils Landegren and Donald Sharon contributed equally to the work

Affiliations

[1]Department of Medicine (Solna), Karolinska University Hospital, Karolinska Institutet, Sweden

[2]Science for Life Laboratory, Department of Medical Sciences, Uppsala University, Sweden

[3]Department of Genetics, Stanford University, California, USA

[4]Department of Molecular, Cellular, and Developmental Biology, Yale University, Connecticut, USA

[5]Department of Medical Sciences, Cancer Pharmacology and Computational Medicine, Uppsala University

[6]Bioinformatics Infrastructure for Life Sciences

[7]Department of Immunology, Genetics and Pathology, Uppsala University, Sweden and Science for Life Laboratory

[8] Department of Molecular Medicine and Surgery, Karolinska Institutet, Stockholm, Sweden

[9]Department of Endocrinology and Department of Medical and Health Sciences and Department of Clinical and Experimental Medicine, Linköping University, Linköping, Sweden

[10]Integrative Reproductive Medicine Group, Intramural Research Program on Reproductive and Adult Endocrinology, National Institute of Child Health and Human Development, National Institutes of Health, Bethesda, MD 20892, USA.

[11]Department of Women's and Children's Health*, Uppsala University, Sweden*

[12]Department of Clinical Science, University of Bergen, and Department of Medicine, Haukeland University Hospital, Bergen, Norway

[13]Diabetes Center, University of California San Francisco, USA

*Correspondence should be addressed to

Nils Landegren

nils.landegren@ki.se

Department of Medicine Solna, Karolinska Institute

Experimental endocrinology

Center for Molecular Medicine, L8:01, Karolinska University Hospital

SE-171 76 Stockholm

nils.landegren@ki.se

phone: +46851779158

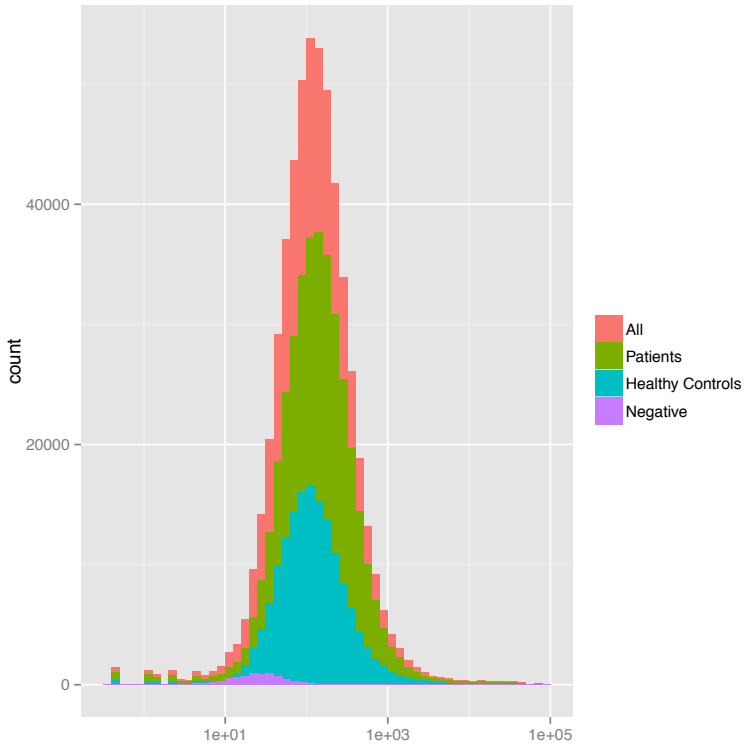

Fig. S1. Distribution of log-intensities for arrays probed with patient sera, healthy control sera or without serum sample (Negative).

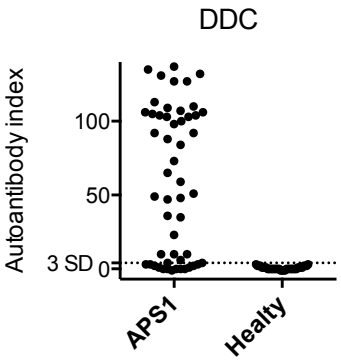

Fig. S2. The proteome array results for DDC autoantibody detection were validated using a radio-ligand binding assay (RLBA) in the 51 patients from the APS1 discovery cohort and in 39 healthy controls. The upper limit of the normal range was defined as three standard deviations above the average of the healthy controls.

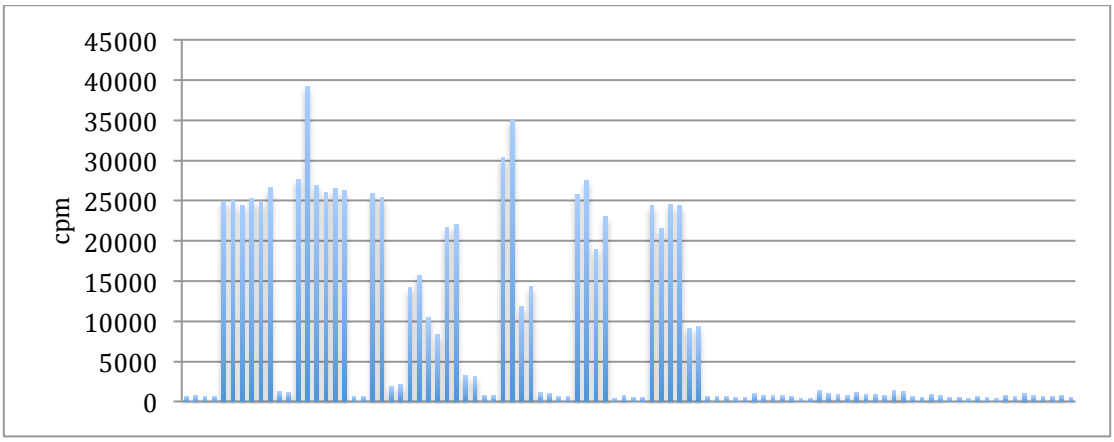

Fig. S3. Representative raw data from the DDC autoantibody radio-ligand binding assay. All patient and control samples were analyzed in duplicate. Negative control (bar 1-4), positive control (bar 5-8), patients with APS1 (bar 9-68) and healthy control subjects (bar 69-96). Counts per minute (CPM).

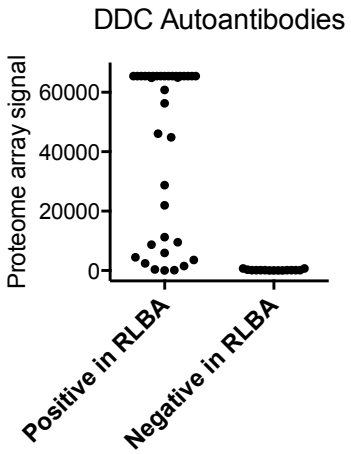

Fig. S4. The proteome array results for DDC were compared against the results from the radio-ligand binding assay (RLBA) for the 51 patients in the APS1 discovery cohort. Patients who were positive for DDC autoantibodies in the RLBA are grouped to the left (cut-off = average of the healthy + 3SD). Proteome array signals are

represented as the average fluorescence signal intensities for protein duplicates on the array after subtraction of the background signal.

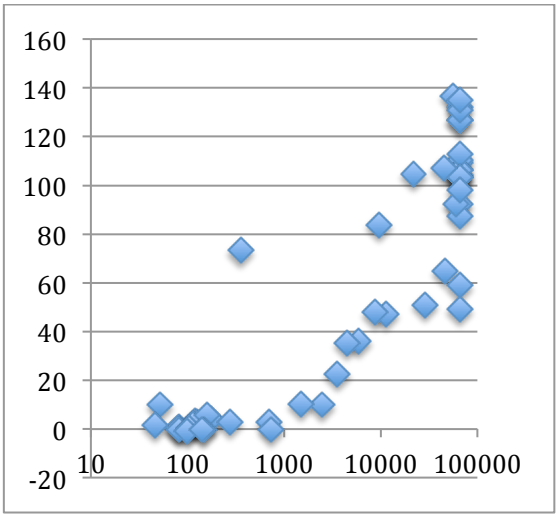

Fig. S5. The proteome array results for DDC were compared against the results from the radio-ligand binding assay (RLBA) for the 51 patients in the APS1 discovery cohort. Proteome array signal results are shown on the x-axis and RLBA results on the y-axis. Proteome array signals are represented as the average fluorescence signal intensities for protein duplicates on the array after subtraction of the background signal. RLBA results are shown as autoantibody index values.

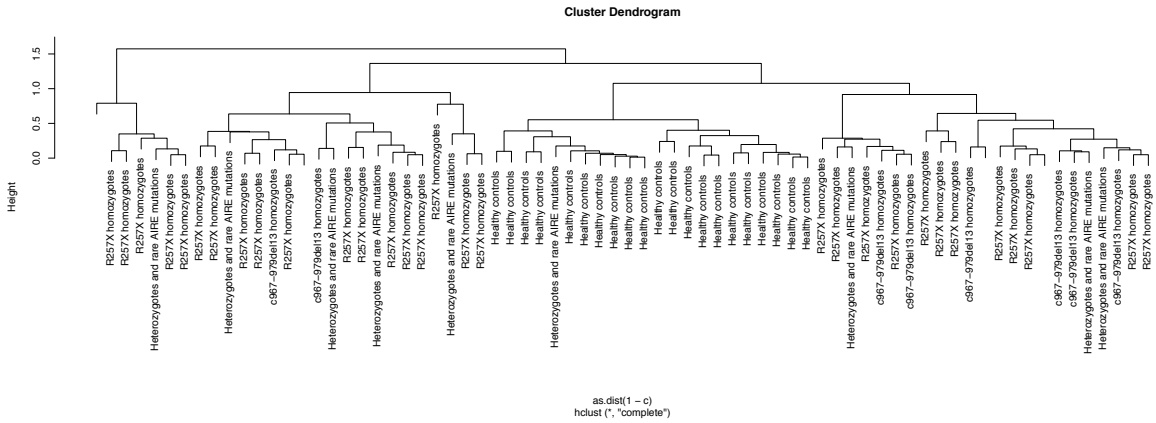

Fig. S6. Patients with APS1 and healthy controls were clustered based on Spearman correlations for the known autoantigens; glutamate decarboxylase 2 (GAD2), glutamate decarboxylase 1 (GAD1), tryptophan hydroxylase (TPH1), aromatic L-amino acid decarboxylase (DDC), gastric intrinsic factor (GIF), cytochrome P450, family 1, subfamily A, polypeptide 2 (CYP1A2), potassium channel regulator (KCNRG), testis specific 10 (TSGA10), interleukin 22 (IL22), interleukin 17A (IL17A), interferon omega (IFNW1) and interferon alpha 1 (IFNA1). Distance = 1 – correlation.

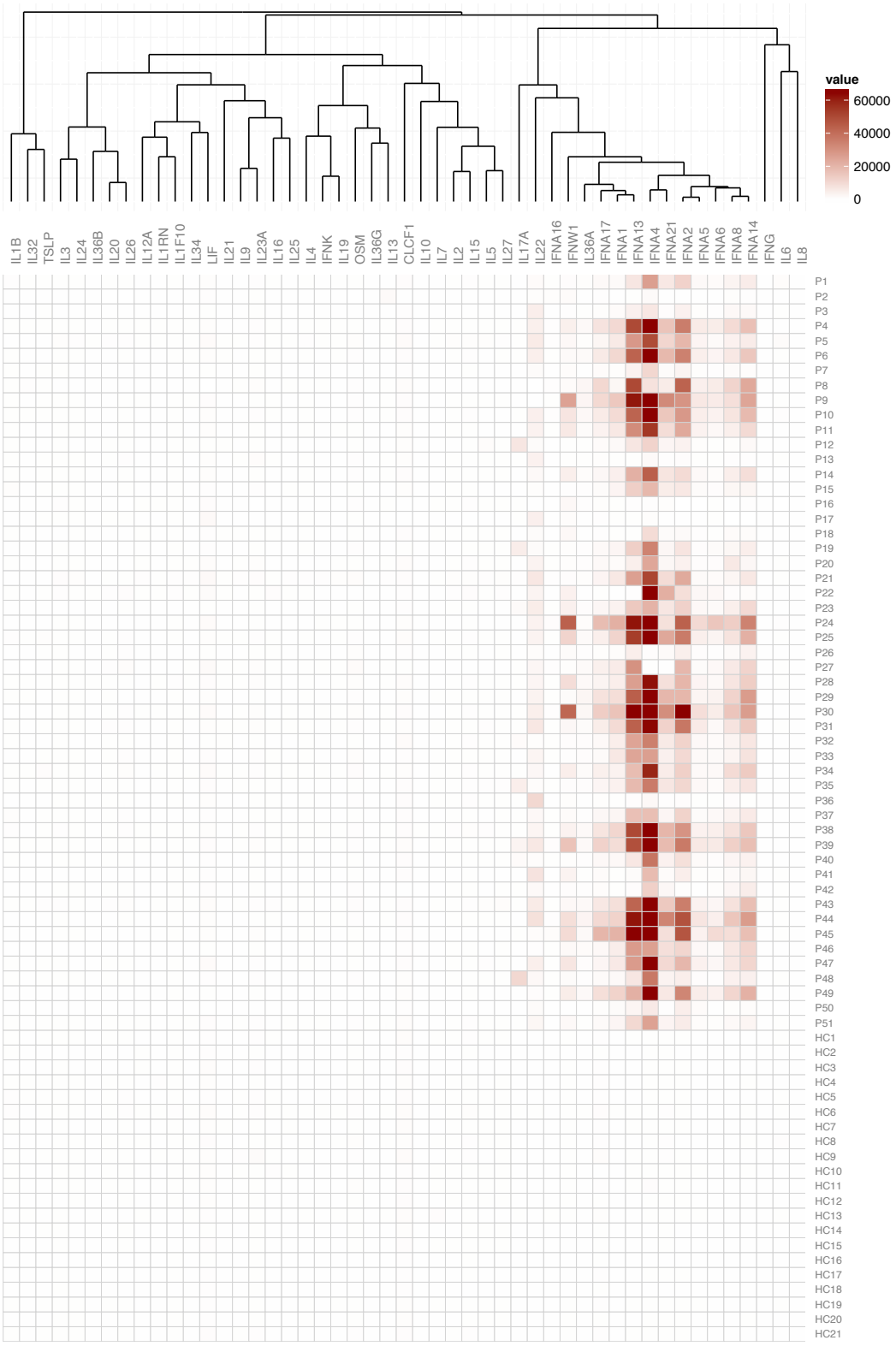

Fig. S7. Focused investigation of 49 interferons, interleukins and other closely related cytokines. High autoantibody signals were seen specifically for the previously

established immune targets, including multiple alpha interferon specifies, IFNW1, IL22 and IL17A (IL17F was not present in the array panel)

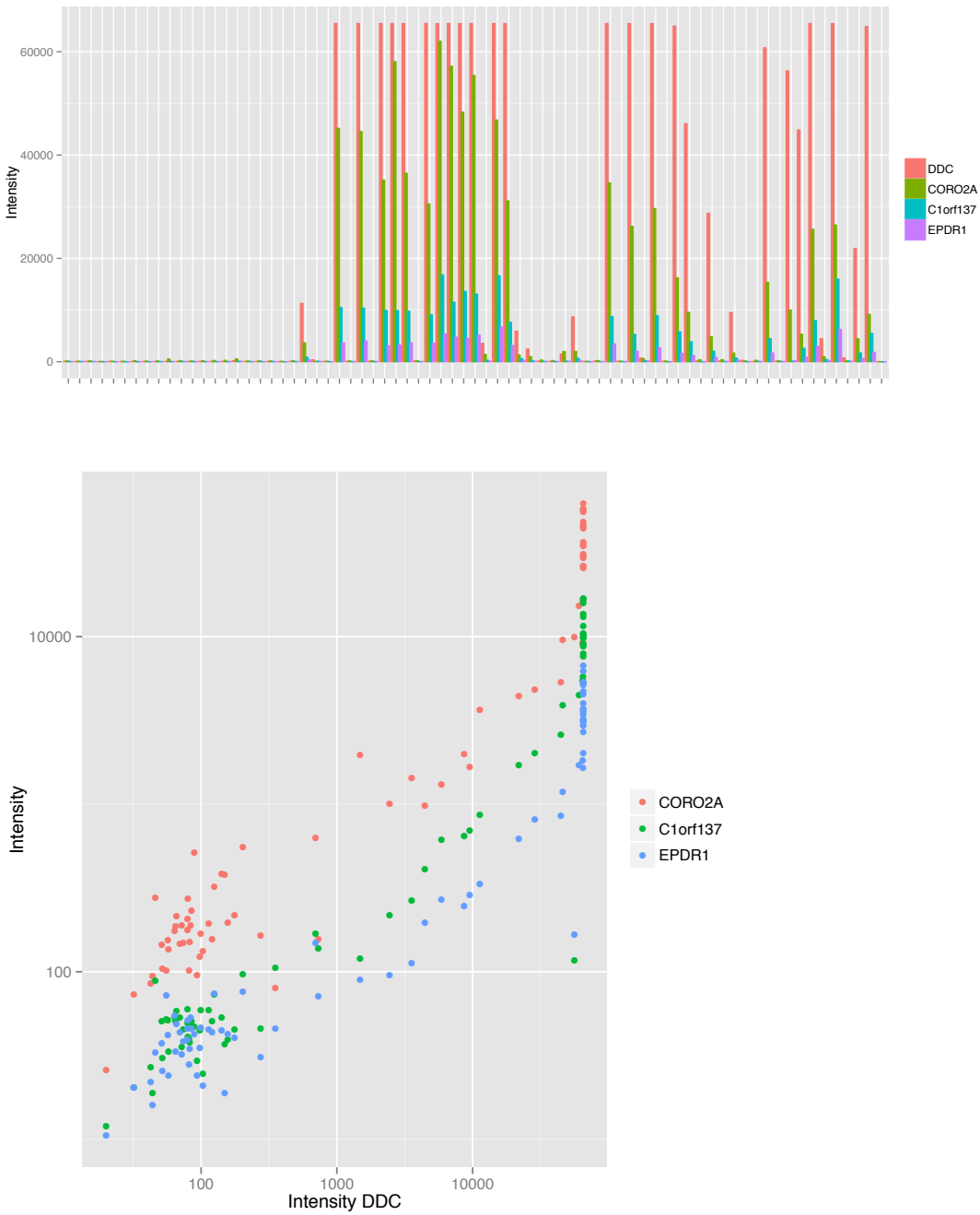

Fig. S8. Printing contamination artifacts exemplified by DDC and adjacent targets. Correlated protein array signals between DCC, an established APS1 autoantigen, and

nearby located proteins; CORO2AA, C1orf137 and EPDR1. Healthy subjects (n=21) are grouped to the left and patients with APS1 (n=51) to the right in the upper image. Average fluorescence signal intensities for protein duplicates on the array after subtraction of the background signal are shown.

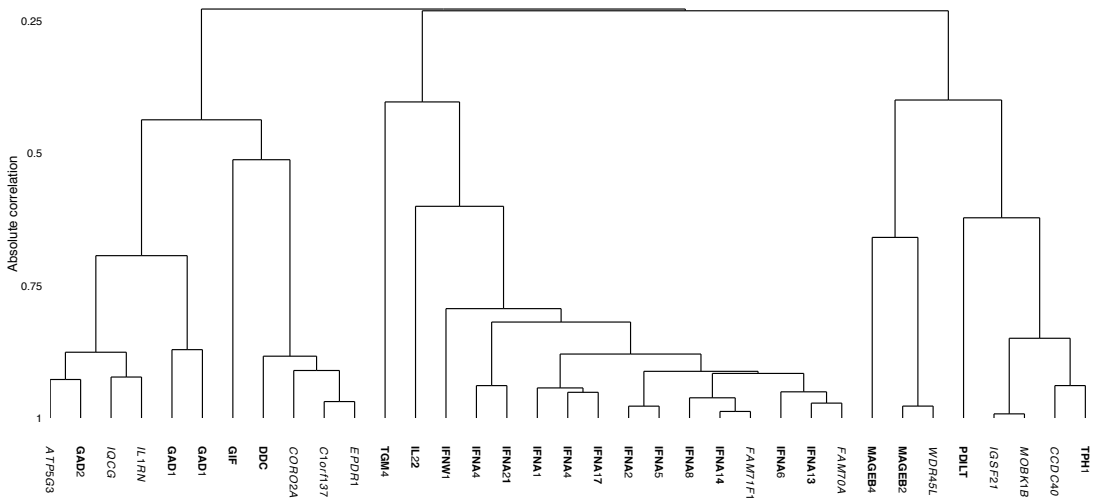

Fig. S9. Identification of printing contamination artifacts in the proteome array data set. Correlations between the top targets in the protein array screen before annotation are shown. Unexpected strong correlations between targets closely located on the array were identified as artifacts (marked in Italic) and excluded from the analyses.

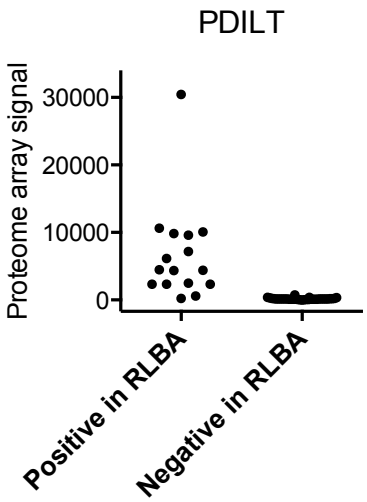

Fig. S10. Validation of PDILT autoantibodies in the APS1 discovery cohort (n=51) using a radio-ligand binding assay (RLBA). Patients that were positive for PDILT autoantibodies in the RLBA are grouped to the left. The cut-off in the RLBA was defined as an index-value of 15. Proteome array signals are shown as the average fluorescence signal intensities for protein duplicates on the array after subtraction of the background signal.

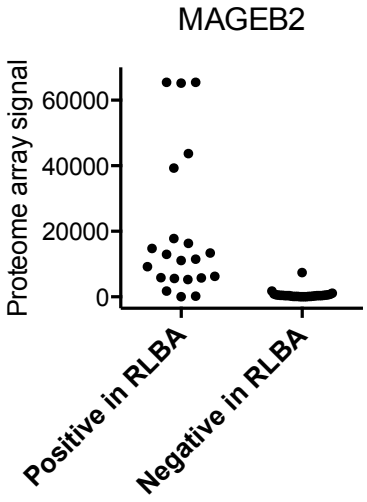

Fig. S11. Validation of MAGEB2 autoantibodies in the APS1 discovery cohort (n=51) using a radio-ligand binding assay (RLBA). Patients that were positive for MAGEB2

autoantibodies in the RLBA are grouped to the left. The cut-off in the RLBA was defined as an index-value of 15. Proteome array signals are shown as the average fluorescence signal intensities for protein duplicates on the array after subtraction of the background signal.

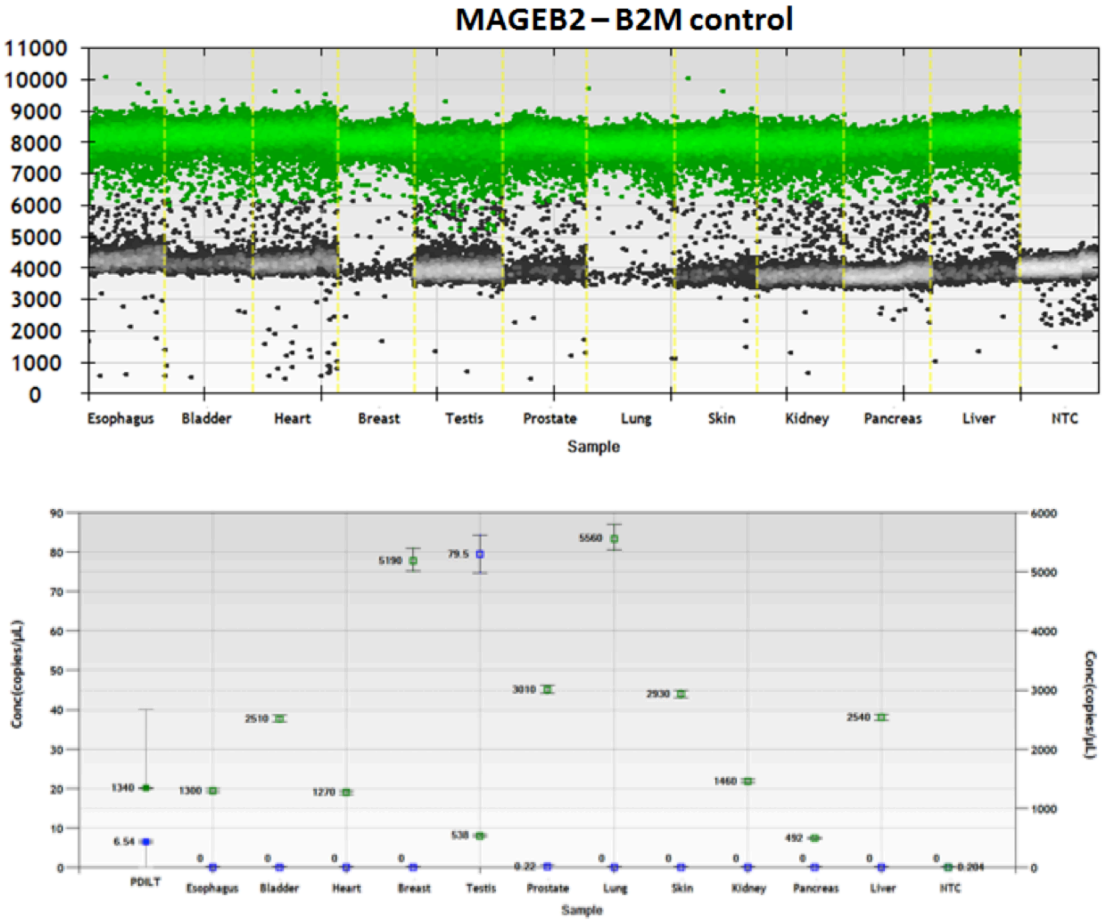

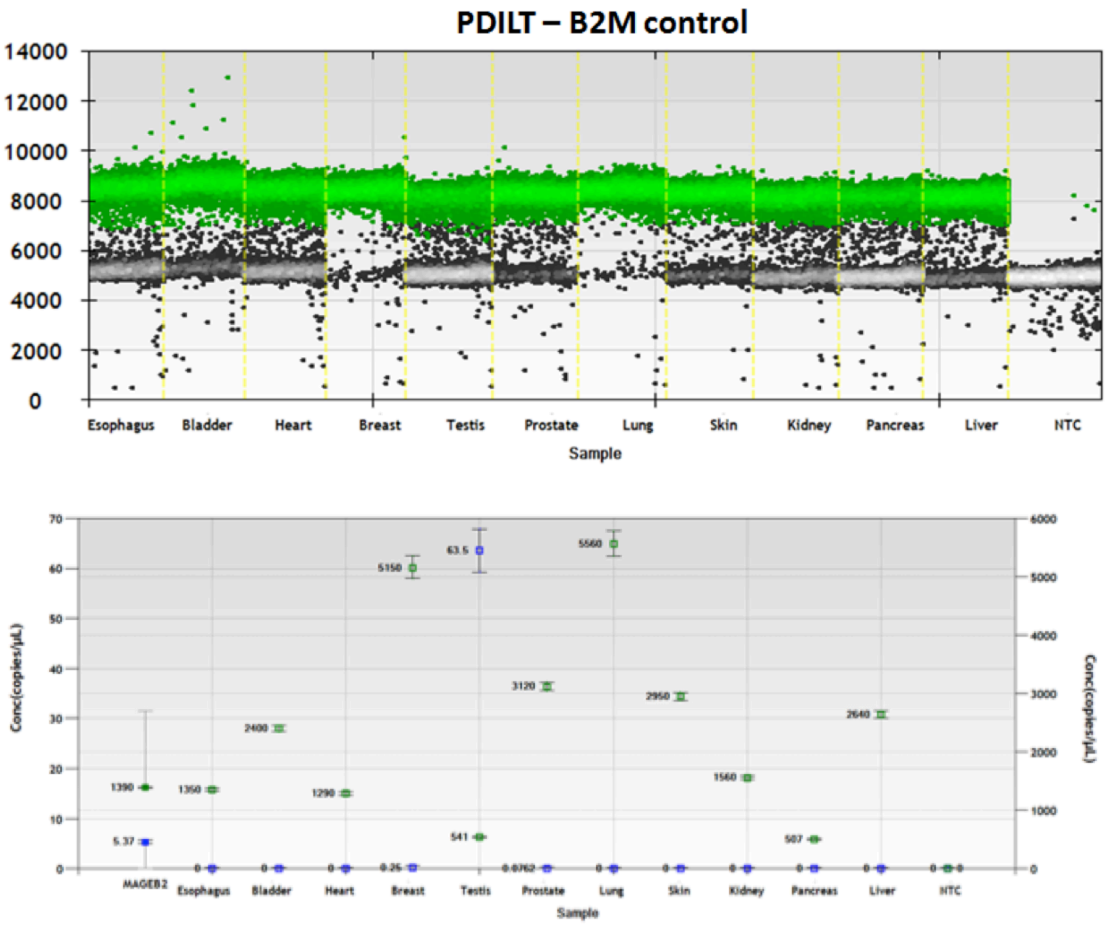

Fig. S12. mRNA levels of MAGEB2 and PDILT were assessed in multiple human tissues by digital droplet PCR. The greatest number of high amplitude events is seen in the testis cDNA sample, and very few or no high amplitude events are seen for the other tissue samples and the *no template control* (NTC). Grey dots denote events with intensities below cut-off. The results for PDILT and MAGEB2 were compared against that of β2M.

Autoantigen	Prevalence	
IFNW1	47/51	92%
IFNA1	46/51	90%
DDC	37/51	73%
IL22	35/51	67%
TPH1	28/51	55%
GAD2	22/51	43%
GAD1	15/51	29%
GIF	14/51	27%
IL17A	12/51	24%
KCNRG	3/51	6%
CYP1A2	2/51	4%
TSGA10	2/51	4%

Table S1. Prevalence of established autoantibodies in the protein array screen. 51 patients with APS1 were investigated. The upper limit of the normal range was defined as three standard deviations above the average of the healthy control subjects.

Gene	Tissue expression, mRNA seq (HPA)
TPH1	Group enriched (colon, duodenum, rectum, small intestine, stomach).
DDC	Tissue enhanced (duodenum, kidney, small intestine).
GAD2	Tissue enriched (cerebral cortex).
GAD1	Tissue enriched (cerebral cortex).
IFNA13	Not detected.
IL22	Not detected.
GIF	Tissue enriched (stomach).
MAGEB2	Tissue enriched (testis).
MAGEB4	Tissue enriched (testis).
PDILT	Group enriched (stomach, testis).
TGM4	Tissue enriched (prostate).

Table S2. Tissue expression profiles of the major immune targets in the proteome array screen. mRNA sequencing data on gene expression profiles obtained from the Human Protein Atlas, http://www.proteinatlas.org. For comparison, among 20,344 genes investigated by the Human Protein Atlas, 2,355 (12%) were classified as being *Tissue enriched*, 1,109 as *Group enriched* (5%), 3,478 (17%) as *Tissue enhanced*, 8,874 (44%) as *Expressed in all*, 2,696 (13%) as *Mixed* and 1,832 (9%) as *Not detected* [39]. Several type 1 interferon species were major immune targets in the patients with APS1 but are here represented by IFNA13 only.

Best GOs	GO description	Genes	Group count	Total count	P-value (Benjamini corrected)
GO:0042136	neurotransmitter biosynthetic process	TPH1 GAD2 GAD1	3	16	1.05e-05
GO:0006540	glutamate decarboxylation to succinate	GAD2 GAD1	2	2	1.23e-05
GO:0006105	succinate metabolic process	GAD2 GAD1	2	2	1.23e-05
GO:0004351	glutamate decarboxylase activity	GAD2 GAD1	2	2	1.23e-05
GO:0042133	neurotransmitter metabolic process	TPH1 GAD2 GAD1	3	32	1.86e-05
GO:0006538	glutamate catabolic process	GAD2 GAD1	2	3	2.47e-05
GO:0016831	carboxy-lyase activity	GAD2 DDC GAD1	3	56	7.37e-05
GO:0005615	extracellular space	IFNW1 IL22 IL17A GIF IFNA13	5	528	7.96e-05
GO:0006519	amino acid and derivate metabolic process	IL22 TPH1 GAD2 DDC GAD1	5	548	8.48e-05
GO:0019842	vitamin binding	GAD2 GIF DDC GAD1	4	245	9.17e-05
GO:0001505	regulation of neurotransmitter levels	TPH1 GAD2	3	78	0.000117

		GAD1			
GO:0009308	amine metabolic process	IL22 TPH1 GAD2 DDC GAD1	5	636	0.000117
GO:0007267	cell-cell signaling	IL22 IL17A TPH1 GAD2 GAD1	5	640	0.000117
GO:0016830	carbon-carbon lyase activity	GAD2 DDC GAD1	3	82	0.000117
GO:0005132	interferon-alpha/beta receptor binding	IFNW1 IFNA13	2	9	0.000118
GO:0006807	nitrogen compound metabolic process	IL22 TPH1 GAD2 DDC GAD1	5	678	0.000134
GO:0005125	cytokine activity	IFNW1 IL22 IL17A IFNA13	4	310	0.000137
GO:0019752	carboxylic acid metabolic process	IL22 TPH1 GAD2 DDC GAD1	5	795	0.000238
GO:0006082	organic acid metabolic process	IL22 TPH1 GAD2 DDC GAD1	5	798	0.000238
GO:0030170	pyridoxal phosphate binding	GAD2 DDC GAD1	3	117	0.000238

GO:0043648	dicarboxylic acid metabolic process	GAD2 GAD1	2	16	0.000268
GO:0006536	glutamate metabolic process	GAD2 GAD1	2	16	0.000268
GO:0044421	extracellular region part	IFNW1 IL22 IL17A GIF IFNA13	5	910	0.000386
GO:0009065	glutamine familty amino acid catabolic process	GAD2 GAD1	2	20	0.000389
GO:0006520	amino acid metabolic process	IL22 TPH1 GAD2 GAD1	4	474	0.00049
GO:0006100	tricarboxylic acid cycle intermediate metabolic process	GAD2 GAD1	2	32	0.000934
GO:0042401	biogenic amine biosynthetic process	TPH1 DDC	2	34	0.000982
GO:0006952	defense response	IFNW1 IL22 IL17A IFNA13	4	584	0.000982
GO:0042398	amino acid derivate biosynthetic process	TPH1 DDC	2	42	0.00145
GO:0016829	lyase activity	GAD2 DDC GAD1	3	278	0.00207

Table S3. Gene ontology terms showing significant overepresentation in established APS1 autoantigens present on the protein array (TPH1, DDC, GAD2, GAD1, IFNA13, IL22, GIF, MAGEB2, MAGEB4, PDILT, TGM4, IFNW1, IL17A, KCNRG, CYP1A2, TSGA10). Associated GO terms were retrieved from the GOa_human database. Minimal length of considered GO paths was set to 3 (default), and top 30 most significant were

reported. 'False discovery rate' according to Benjamini was used for correcting p-values for multiple testing. Results were not clustered.